

Exact quantum algorithm for unit commitment optimization based on partially connected quantum neural networks

Jian Liu(刘键), Xu Zhou(周旭), Zhuojun Zhou(周卓俊), and Le Luo(罗乐)
Citation: Chin. Phys. B, 2025, 34 (**10**): 100303. DOI: 10.1088/1674-1056/adf4aa
http://cpb.iphy.ac.cn; http://iopscience.iop.org/cpb

What follows is a list of articles you may be interested in

Impact of surface passivation on the electrical stability of strained germanium devices

Zong-Hu Li(李宗祜), Mao-Lin Wang(王茂粼), Zhen-Zhen Kong(孔真真), Gui-Lei Wang(王桂磊), Yuan Kang(康原), Yong-Qiang Xu(徐永强), Rui Wu(吴睿), Tian-Yue Hao(郝天岳), Ze-Cheng Wei(魏泽成), Bao-Chuan Wang(王保传), Hai-Ou Li(李海欧), Gang Cao(曹刚), and Guo-Ping Guo(郭国平)
Chin. Phys. B, 2025, 34 (**9**): 090305. DOI: 10.1088/1674-1056/add4de

Domain adaptation method inspired by quantum convolutional neural network

Chunhui Wu(武春辉), Junhao Pei(裴骏豪), Yihua Wu(吴逸华), Anqi Zhang(张安琪), and Shengmei Zhao(赵生妹)
Chin. Phys. B, 2025, 34 (**7**): 070302. DOI: 10.1088/1674-1056/adc7ed

Planar: A software for exact decoding quantum error correction codes with planar structure

Dongyang Feng(冯东阳), Hanyan Cao(曹涵彦), and Pan Zhang(张潘)
Chin. Phys. B, 2025, 34 (**5**): 050311. DOI: 10.1088/1674-1056/adcb26

Distributed quantum circuit partitioning and optimization based on combined spectral clustering and search tree strategies

Zilu Chen(陈子禄), Zhijin Guan(管致锦), Shuxian Zhao(赵书娴), and Xueyun Cheng(程学云)
Chin. Phys. B, 2025, 34 (**5**): 050305. DOI: 10.1088/1674-1056/adbada

All-microwave CZ gate based on fixed-frequency driven coupler

Wanpeng Gao(高万鹏), Xiaoliang He(何潇梁), Zhengqi Niu(牛铮琦), Daqiang Bao(包大强), Kuang Liu(刘匡), Junfeng Chen(陈俊锋), Zhen Wang(王镇), and Z. R. Lin(林志荣)
Chin. Phys. B, 2025, 34 (**4**): 040304. DOI: 10.1088/1674-1056/adb68a

---

Exact quantum algorithm for unit commitment optimization based on partially connected quantum neural networks

Jian Liu(刘键)[2,†], Xu Zhou(周旭)[1,3,6,†,‡], Zhuojun Zhou(周卓俊)[2], and Le Luo(罗乐)[1,4,5]

[1] *School of Physics and Astronomy, Sun Yat-Sen University, Zhuhai* 519082, *China*
[2] *QUDOOR Co., Ltd., Hefei* 230000, *China*
[3] *QUDOOR Co., Ltd., Beijing* 100089, *China*
[4] *Shenzhen Research Institute of Sun Yat-Sen University, Shenzhen* 518057, *China*
[5] *Guangdong Provincial Key Laboratory of Quantum Metrology and Sensing, Sun Yat-Sen University, Zhuhai* 519082, *China*
[6] *Yangtze Delta Industrial Innovation Center of Quantum Science and Technology, Suzhou* 215000, *China*

(Received 2 December 2024; revised manuscript received 14 July 2025; accepted manuscript online 28 July 2025)

The quantum hybrid algorithm has recently become a very promising and speedy method for solving larger-scale optimization problems in the noisy intermediate-scale quantum (NISQ) era. The unit commitment (UC) problem is a fundamental problem in the field of power systems that aims to satisfy the power balance constraint with minimal cost. In this paper, we focus on the implementation of the UC solution using exact quantum algorithms based on the quantum neural network (QNN). This method is tested with a ten-unit system under the power balance constraint. In order to improve computing precision and reduce network complexity, we propose a knowledge-based partially connected quantum neural network (PCQNN). The results show that exact solutions can be obtained by the improved algorithm and that the depth of the quantum circuit can be reduced simultaneously.

Keywords: quantum computing, quantum algorithm, unit commitment, quantum neural network, noisy intermediate-scale quantum era

PACS: 03.67.Ac, 03.67.Lx, 88.50.Mp, 45.10.Db

DOI: 10.1088/1674-1056/adf4aa **CSTR:** 32038.14.CPB.adf4aa

1. Introduction

Unit commitment (UC) is a critically important optimization problem in the field of electrical power systems, which aims to meet the user's demand for electric energy by rationally scheduling the generator sets in the power system. The problem addressed by UC is to determine the most appropriate power-unit startup and shutdown schedule to minimize the cost of power generation while meeting a large number of operating and security constraints. It is a nonlinear mixed-integer quadratic program (MIQP) with both continuous and integer variables. The treatment of the binary commitment decision variables induces large combinatorial complexity. Numerous methods, such as those described in Refs. [1,2], have been employed to tackle this NP-hard problem. While algorithms like branch-and-bound theoretically offer optimal solutions to the UC problem, their application in large-scale systems is limited due to extensive computation times. Other approaches, including priority lists[3] and Lagrangian relaxation,[4] do not guarantee optimal solutions. Hybrid algorithms, such as genetic algorithms[5] and machine learning,[6] have been proposed to combine different methods and enhance solution quality.

Although quantum algorithms for optimization problems have made significant progress in recent years, the number of qubits in quantum computers is still limited. Thus, finding ways to solve larger-scale problems in the noisy intermediate-scale quantum (NISQ) era has become one of the most urgent tasks. The design, implementation, and application of new quantum algorithms for larger systems have become the focus of attention. Variational quantum algorithms (VQAs)[7] are among the most promising schemes within the class of NISQ algorithms, including the variational quantum eigensolver (VQE),[8] the quantum approximate optimization algorithm (QAOA),[9] quantum neural networks (QNNs),[10–14] etc. VQA has been developed for a wide range of applications, including calculating molecular ground states, dynamically simulating many-body systems, and solving linear equations. Recently, the VQE algorithm and the QAOA[15–18] were both proposed to tackle the UC problem. To deal with continuous variables, some classical methods have been combined with the quantum algorithm, such as the alternating direction method of multipliers (ADMM),[19] Benders decomposition,[20] etc. It is well known that classical algorithms are very efficient in handling continuous variable optimization problems, with the majority of the time (80%–90%) being consumed in the optimization process of integer variables. Therefore, if quantum acceleration is to be achieved,

[†]These authors contributed equally to this work.
[‡]Corresponding author. E-mail: zhoux359@mail.sysu.edu.cn

© 2025 Chinese Physical Society and IOP Publishing Ltd. All rights, including for text and data mining, AI training, and similar technologies, are reserved.

the research focus should be on utilizing quantum algorithms to achieve integer optimization.

In our research, we propose the knowledge-based partially connected quantum neural network (PCQNN) algorithm to achieve optimal efficiency in solving the UC problem. The PCQNN can be defined as a QNN that contains only a subset of the possible connections within a given QNN model, which comes from a partially connected neural network (PCNN). Fully connected neural networks (FCNNs) are prevalent in classical neural network applications. However, they often include a significant amount of redundancy. In contrast, a PCNN is characterized by a network that includes only a subset of the potential connections present in a complete neural network model, as surveyed in Ref. [21]. The concept of the PCQNN is to simplify the topology of a QNN using symbolic domain knowledge. This approach aims to enhance the performance of a hardware-efficient ansatz (HEA) model while utilizing a reduced number of connections, thereby increasing computational efficiency.

In Section 2, we initially construct the theoretical framework for the optimization problem, including both equality and inequality constraints. Subsequently, the UC problem is translated into an interactional Ising Hamiltonian model. Moving to Section 3, we detail the QNN circuit designed for a ten-unit system with single constraint optimization. Following this, we introduce a problem-inspired PCQNN circuit for a five-unit system with double constraint optimization. Our findings presented in Section 4 demonstrate that, similar to PCNNs in classical computing, the PCQNN circuit can achieve higher precision with shallower circuit depth in quantum optimization tasks. Consequently, our research proposes an accurate algorithm that is well-suited for the UC problem, particularly in distributed quantum computing environments. Moreover, this methodology is not confined to UC problems; it possesses the potential to be extended to a broad spectrum of combinatorial optimization problems.

2. Theoretical framework

A general optimization problem can be written mathematically as follows:

$$\text{minimize} \quad f_0(x), \tag{1}$$

$$\text{subject to} \quad f_{i,\text{eq}}(x) = A_i, \quad i \in [l], \tag{2}$$

$$f_{i,\text{neq}}(x) \le B_i, \quad i \in [m], \tag{3}$$

where $f_0 : \boldsymbol{R}^n \to \boldsymbol{R}$ is the objective function, $f_{i,\text{eq}}, f_{i,\text{neq}} : \boldsymbol{R}^n \to \boldsymbol{R}$ are equality and inequality constraints, respectively, $x = (x_1, x_2, \ldots, x_n)$ are optimization binary variables with domains of $x_i \in \{0,1\}$, and A_i and B_i are constants. The numbers of equality and inequality constraints are l and m, respectively. The main parameters used in this paper are shown in Table 1.

The optimization problem should be transformed into a quadratic unconstrained binary optimization (QUBO) problem based on the Hamiltonian of the Ising model so that it can be solved by a quantum computer:

$$H = \sum_{i=1}^{n} \mathcal{C}_{ii} Z_i + \sum_{1 \le i < j \le n}^{n} \mathcal{C}_{ij} Z_i Z_j, \tag{4}$$

where $\mathcal{C}_{ii}$ and $\mathcal{C}_{ij}$ are undetermined coefficients and Z_i and Z_j are Pauli operators for spin qubits. This process can be achieved using the following steps.

Transform inequality constraints into equality constraints by adding relaxation variables s_i:

$$f_{i,\text{neq}}(x) - B_i + s_i = 0, \tag{5}$$

where the integer variables s_i can be represented efficiently as a binary problem that requires a logarithmic number of binary variables:

$$s_i = \sum_{q=n+1}^{n+k} 2^{q-n-1} x_q. \tag{6}$$

A integer variable s_i ranging from 0 to N can be represented using

$$k = \log_2 N \tag{7}$$

binary variables x_j. Hence, additional k qubits are used to represent the relaxation variable s_i.

Obtain a QUBO problem by penalty function methods,

$$f_0(x) + \sum_{i=1}^{l} \lambda_1 (f_{i,\text{eq}}(x) - A_i)^2 + \sum_{i=1}^{m} \lambda_2 (f_{i,\text{neq}}(x) - B_i + s_i)^2, \tag{8}$$

where λ_i is the weight of the penalty function.

Table 1. Parameters used in this paper.

Symbol	Description	Symbol	Description
f_0	objective function	a_i	quadratic coefficients
$f_{i,\text{eq}}$	equality constraints	b_i	linear coefficients
$f_{i,\text{neq}}$	inequality constraints	c_i	opening costs
x_i	binary variables	p_i	power of i-th unit
H	Hamiltonian	L	total load
Z_i	Pauli Z operators	S	system spare power
s_i	relaxation variables	θ	variational parameters
n	number of unit qubits	θ^*	optimization parameters
k	number of auxiliary qubits	d	number of layers
λ_i	weight of penalty functions	$p_{i,\max}$	maximum power of i-th unit

Transform binary variables into spin by

$$x_i = \frac{I - Z_i}{2}, \quad i = 1, \ldots, n+k, \tag{9}$$

where Z_i is the Pauli Z operation. By substituting Eq. (9) into Eq. (8), a Hamiltonian in the form of Eq. (4) can be obtained by calculation.

From Eq. (6), we find that, in order to deal with the relaxation variables s_i, one needs k auxiliary qubits. Thus, inequality constraints may induce additional complexity within

the computation. In order to reduce the number of auxiliary qubits, it is necessary to proceed on a case-by-case basis.

Specifically, the UC solution determines the combination of units' on/off statuses that meets the load requirements in a given time period. For a single time period, the objective function shall be the sum of the costs of the operating generator units,

$$\sum_{i=1}^{n} f_i x_i = \sum_{i=1}^{n} (a_i p_i^2 + b_i p_i + c_i) x_i, \tag{10}$$

where a_i, b_i, and c_i are the fixed cost coefficients of the i-th unit.

For an n-unit power system, the system power balance shall be preserved by an equality constraint

$$\sum_{i=1}^{n} p_i x_i = L, \tag{11}$$

where L is the total load. The system spare constraint can be expressed by the following inequality:

$$\sum_{i=1}^{n} p_{i,\max} x_i \geq L + S, \tag{12}$$

where S is the system spare power. The up and down power constraints can be expressed as

$$p_{i,\min} x_i \leq p_i \leq p_{i,\max} x_i. \tag{13}$$

Transform inequality constraints into equality constraints by adding relaxation variables,

$$\sum_{i=1}^{n} p_{i,\max} x_i - L - S = 0, \tag{14}$$

$$p_i - p_{i,\max} x_i + S_{i,\max} = 0, \tag{15}$$

$$p_i - p_{i,\min} x_i - S_{i,\min} = 0, \tag{16}$$

where the relaxation variables S, $S_{i,\max}$, and $S_{i,\min}$ can be expressed using binary numbers, as shown in Eq. (6).

By transforming the constraints (here, we consider the power balance and system spare constraints) into penalty functions and using the binary-spin transformation, we can obtain the Hamiltonian for our specific problem

$$\begin{aligned} H = & \sum_{i=1}^{n} f_i \left(\frac{I - Z_i}{2} \right) + \lambda_1 \left(\sum_{i=1}^{n} p_i \left(\frac{I - Z_i}{2} \right) - L \right)^2 \\ & + \lambda_2 \left(\sum_{i=1}^{n} p_{i,\max} \left(\frac{I - Z_i}{2} \right) - L - S \right. \\ & \left. - c_c \sum_{q=n+1}^{n+k} 2^{q-n-1} \left(\frac{I - Z_q}{2} \right) \right)^2, \end{aligned} \tag{17}$$

where c_c is a constant determined by the magnitude of relaxation variables. We refer to the first n qubits that represent the on/off statuses of the generators as on/off qubits, and we refer to the subsequent k qubits that represent the relaxation variables as auxiliary qubits.

3. Quantum algorithm for UC

In this section, we first describe how a basic QNN works and then introduce the PCQNN circuit for the UC problem.

3.1. Quantum neural networks

The way in which an HEA QNN processes data is as follows: Encode the input data into the corresponding quantum states using an appropriate number of qubits. The quantum states of all qubits are transformed by passing through parameterized rotation gates and entanglement gates; this is repeated for a given number of layers. Measure the output quantum state to obtain the expectation value of Hamiltonian operators composed of Pauli gates. The parameters are updated by an optimizer, such as the adaptive moment estimation (ADAM) optimizer, the Broyden, Fletcher, Goldfarb, and Shanno (BFGS) algorithm, etc. based on the feedback loop of the QNN circuit. Figure 1 shows an example of a QNN algorithm.

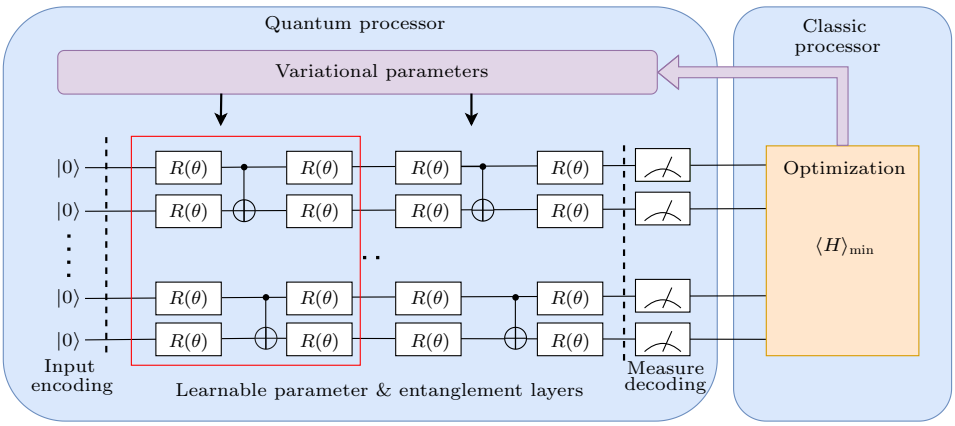


Fig. 1. Diagram of a QNN quantum–classical algorithm. The variational parameters are $\theta = (\theta_1, \theta_2, \ldots)$. The rotation gates R can be decomposed into the 3D rotations R_x, R_y, and R_z. The red frame denotes one repeated layer.

3.2. Knowledge-based PCQNN circuit

In order to improve the efficiency of the circuit operation, we apply the PCQNN using a knowledge-based method. The idea is to use symbolic domain knowledge as rules to actually create the topology of the neural network. Next, the actual neural training quantum algorithm is applied to improve the performance of the network.

We first introduce some parameters for the UC problem, including the total cost $\mathcal{F}$, total power $\mathcal{P}$, total max power $\mathcal{M}$, and the relaxation variable $\mathcal{R}$, which can be defined as

$$\mathcal{F} = \sum_{i=1}^{n} f_i x_i, \tag{18}$$

$$\mathcal{P} = \sum_{i=1}^{n} p_i x_i, \tag{19}$$

$$\mathcal{M} = \sum_{i=1}^{n} p_{i,\max} x_i, \tag{20}$$

$$\mathcal{R} = \sum_{q=n+1}^{n+k} 2^{q-n-1} x_q. \tag{21}$$

Therefore, the Hamiltonian of the UC problem can be rewritten as

$$H = \mathcal{F} + \lambda_1 (\mathcal{P} - L)^2 + \lambda_2 (\mathcal{M} - \mathcal{R} - L - S)^2. \tag{22}$$

We have identified that the initial three parameters are indicative of the physical characteristics of the generator units. These parameters can be determined from the arguments associated with the initial n qubits. In contrast, the last parameter represents the relaxation variable, which can be determined from the subsequent k qubits. Consequently, the UC problem can be approached as an optimization involving the symbolic parameters $\mathcal{F}$ (fuel cost), $\mathcal{P}$ (power output), $\mathcal{M}$ (maintenance), and $\mathcal{R}$ (relaxation).

In fact, the architecture of the PCQNN is directly inspired by that of the classical PCNN. For example, in bird image recognition, when identifying birds with distinctive head features, PCNN may decompose the image into head and body regions, which are processed by separate subnetworks, followed by further training and prediction. This is referred to as a knowledge-based approach — decomposing bird images based on the known characteristics of their heads and bodies and then processing them in parallel or jointly using classical neural networks.

Similarly, one can input the generator's properties and the relaxation variable into the network as two distinct sets of data. Subsequently, the information from these two inputs can be integrated at the end of the quantum network's processing by a classical optimizer. This approach ensures a balanced focus on both the local details and the overarching system, thereby achieving the desired optimization goals. A simple schematic diagram is shown in Fig. 2.

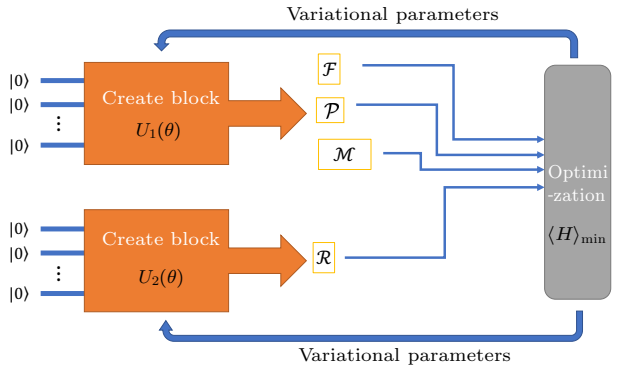


Fig. 2. Diagram of the quantum algorithm of the knowledge-based PCQNN used for the UC problem.

To demonstrate the reason for the PCQNN circuit, we begin with the total Hamiltonian for the UC problem

$$\begin{aligned} H = & \sum_{i=1}^{n} f_i \left(\frac{I - Z_i}{2} \right) + \lambda_1 \left(\sum_{i=1}^{n} p_i \left(\frac{I - Z_i}{2} \right) - L \right)^2 \\ & + \lambda_2 \left(\sum_{i=1}^{n} p_{i,\max} \left(\frac{I - Z_i}{2} \right) - L - S \right. \\ & \left. - c_c \sum_{q=n+1}^{n+k} 2^{q-n-1} \left(\frac{I - Z_q}{2} \right) \right)^2. \end{aligned} \tag{23}$$

For clarity, we decompose the Hamiltonian into its fundamental components

$$H_{\mathrm{I}}^{(1)} = \sum_{i=1}^{n} f_i \left(\frac{I - Z_i}{2} \right),$$

(generator operating cost term), (24)

$$H_{\mathrm{I}}^{(2)} = \sum_{i=1}^{n} p_i \left(\frac{I - Z_i}{2} \right),$$

(real-time power balance term), (25)

$$H_{\mathrm{I}}^{(3)} = \sum_{i=1}^{n} p_{i,\max} \left(\frac{I - Z_i}{2} \right),$$

(maximum power constraint term), (26)

$$H_{\mathrm{II}} = c_c \sum_{q=n+1}^{n+k} 2^{q-n-1} \left(\frac{I - Z_q}{2} \right),$$

(auxiliary variable encoding term). (27)

The total Hamiltonian can then be expressed in tensor product form as

$$\begin{aligned} H = & \underbrace{\left(\sum_{i=1}^{3} \varepsilon_i H_{\mathrm{I}}^{(i)} \otimes I + \sum_{i=2}^{3} \eta_i H_{\mathrm{I}}^{(i)} \otimes H_{\mathrm{I}}^{(i)} \right)}_{\text{Subsystem A terms}} \\ & + \underbrace{(\rho_1 H_{\mathrm{II}} \otimes I + \rho_2 H_{\mathrm{II}} \otimes H_{\mathrm{II}})}_{\text{Subsystem B terms}} + \underbrace{\gamma H_{\mathrm{I}}^{(3)} \otimes H_{\mathrm{II}}}_{\text{A–B interaction}} + \text{Const.}, \end{aligned} \tag{28}$$

where the Greek letters ε_i, η_i, ρ_i, and γ represent the coefficients of the expanded terms. The total Hamiltonian can be decomposed into the independent terms of subsystem A (on/off qubits), those of subsystem B (auxiliary qubits), and their interaction terms. The term $\sum_{i=1}^{3} \varepsilon_i H_{\mathrm{I}}^{(i)} \otimes I$, $\sum_{i=2}^{3} \eta_i H_{\mathrm{I}}^{(i)} \otimes H_{\mathrm{I}}^{(i)}$

acts only on on/off qubits. The term $\rho_1 H_{\rm II} \otimes I$, $\rho_2 H_{\rm II} \otimes H_{\rm II}$ acts only on auxiliary qubits. The interaction term between A and B is $\gamma H_{\rm I}^{(3)} \otimes H_{\rm II}$.

First, all operators $H_{\rm I}^{(i)}$ $(i = 1,2,3)$ commute in subsystem A; this ensures the existence of a common eigenstate basis. Second, because any two Ising Hamiltonians composed solely of σ^z interactions commute, $H_{\rm I}^{(3)}$ and $H_{\rm II}$ commute with each other and share common eigenstates ($|\psi_A\rangle$, $|\psi_B\rangle$) in their respective subsystems. The action of the term remains a tensor product state $|\psi_A\rangle \otimes |\psi_B\rangle$, introducing no entanglement.

The total wave function can be expressed as a tensor product state of the two subsystems without entanglement $|\psi\rangle = |\psi_A\rangle \otimes |\psi_B\rangle$ because the $H_{\rm I}^{(i)}$ and $H_{\rm II}$ in the Hamiltonian commute within their respective subsystems and can be simultaneously diagonalized. This ensures that all interaction terms are diagonal in the tensor product basis, preserving the tensor product state structure.

Building upon this theoretical analysis, we demonstrate that the CNOT gates connecting distinct qubit types can be systematically eliminated. This reveals an important design principle: constraint-encoding quantum networks should prioritize interaction modeling over indiscriminate entanglement creation. This derivation is fundamentally rooted in the Hamiltonian analysis that takes place prior to quantum circuit construction. This approach establishes an architecture that we term a knowledge-based PCQNN architecture.

Furthermore, following the above principles, the system can be further partitioned into more subsystems. However, such partitioning would lead to an even more complex interaction structure in the Hamiltonian. When designing quantum algorithms, we must seek an optimal balance between the physical implementation complexity of quantum circuits and the theoretical complexity of the Hamiltonian. This balancing point should be determined with the goal of maximizing computational efficiency.

Although, from a strictly mathematical perspective, we have yet to establish a universal quantitative relationship between Hamiltonian complexity and computational efficiency, it can still be physically understood as follows: as the number of partitioned subsystems in the Hamiltonian increases, the interaction structure becomes increasingly complex. This allows for greater optimization of CNOT gates in the quantum circuit but simultaneously leads to degradation of the circuit's expressive power. This phenomenon reveals a critical trade-off — an optimal balance must be sought between the expressive power of the quantum circuit and its computational efficiency. Specifically, excessive CNOT gates increase circuit complexity and thus reduce computational efficiency, while excessive subsystem partitioning, although reducing the number of CNOT gates, weakens the circuit's expressive power. Specifically, reducing the use of multiqubit gates, namely, CNOT gates, is more conducive for experimental physicists aiming to verify our proposed quantum algorithms in physical systems. This represents a small but significant step toward the practical application of quantum computing. Empirical studies and numerical simulations of the specific UC problem will demonstrate the clear advantages of our proposed optimization approach.

For $n = k = 6$, this model can be treated as double-layer coupled graphene,[23,24] as shown in Fig. 3. Thus, one can use the upper quantum network block to create the upper layer and the lower quantum network block to create the lower layer.

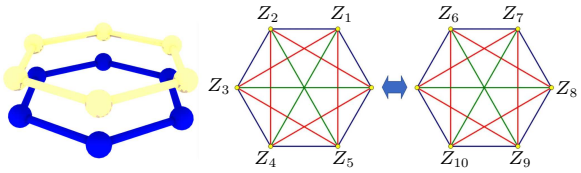


Fig. 3. Diagram of coupled double-layer graphene (left) and a coupled Ising model (right).

The primary motivation behind PCNNs is to achieve a network topology that is either equivalent to or superior in performance compared to fully connected models, while significantly reducing the number of connections. By minimizing the number of connections, PCNNs can enhance generalization capabilities, simplify network complexity, and decrease hardware and storage requirements, as well as training and recall times. Three main classes of methods are used to implement PCNNs: non-ontogenic methods, ontogenic methods, and hybrid methods. Hybrid methods integrate neural networks with other artificial intelligence (AI) techniques, such as symbolic knowledge representation and genetic programming. Specifically, symbolic knowledge methods leverage a knowledge base of domain-specific inference rules (i.e., a domain theory) to guide the network design. For example, in the context of PCQNNs, the first step is to analyze the problem using domain-specific inference rules within the domain theory. Based on this analysis, a quantum circuit is designed. Initially, the problem is mapped onto the interacting Ising model, and the solution is subsequently derived using an equation, (Eq. (28)), which demonstrates that the solution can be expressed as a direct product state without entanglements. This finding allows for a reduction in the number of entangled gates in the PCQNN circuit, thereby optimizing its performance and efficiency.

Therefore, our PCQNN circuit with the problem-inspired ansatz can be obtained by directly removing CNOT gates between the two types of qubits — those representing the unit status and those representing the relaxation variables — from the original HEA QNN circuit (as shown in Fig. 4). Since

$H_{\mathrm{I}}^{(i)}$ and H_{II} can be simultaneously diagonalized in their respective subsystems, their tensor product terms are also diagonal matrices in the tensor product basis, preserving the tensor product state structure. Therefore, they can be generated independently from each other without any entanglement between them. The procedure can be found in Algorithm 1.

Algorithm 1 Knowledge-based PCQNN algorithm

Input:
(1) n : Number of unit nodes
(2) k : Number of auxiliary qubits
(3) p_i : List of powers of the i-th unit
(4) $p_{i,\max}$: List of max powers of the i-th unit
(5) d : Number of layers in the PCQNN
(6) θ_i : List of arguments needed to build the cost layer
Output: The target string $x = (x_1, x_2, \ldots, x_{n+k})$ with high probability
Procedure:
Step 1. Create a list of θ_i parameters
Step 2. Create a list of $n+k$ parameterized rotation gates in three dimensions: R_y, R_z, and R_x
Step 3. Apply the all-zero state to all qubits to initialize the quantum circuit (qc)
Step 4.
$j \leftarrow 1$
while $j \leq d$
  Build and apply a cost layer $U_1(\theta)$ for qubits 1 to n
  Build and apply a cost layer $U_2(\theta)$ for qubits $n+1$ to $n+k$
end while
Step 5. Measure all qubits in the standard basis and store the results in classical registers
Step 6. Use a classical optimizer to find parameters θ^*, to minimize expected cost
End procedure

3.3. Applicability and limitations of PCQNN

Indeed, the UC problem, a mixed-integer programming (MIP) problem, is a typical mathematical optimization problem that includes both equality and inequality constraints. Therefore, if our method in this paper can be applied to the UC problem, it should also be applicable to other optimization problems of similar formation, which can be found at the beginning of Section 2 of this paper.

For example, in the multiple-access-channel problem, the optimization can be expressed as follows:

$$\max \quad \sum_i \log(1+\mathrm{SINR}_i), \tag{29}$$

$$\text{s.t.} \quad 0 < P_i < b_i, \tag{30}$$

where the signal-to-interference-plus-noise ratio (SINR) is given by

$$\mathrm{SINR}_i = \frac{P_i}{\delta_i^2 + \sum_{j\neq i} \alpha_{ij} P_j}, \tag{31}$$

where δ_i is the white noise variance and α_{ij} is the interference caused by the i-th user sending a unit energy signal to the j-th user.

Another example is the well-known portfolio optimization problem,

$$\min_{\boldsymbol{x}} \quad -\boldsymbol{\mu}^{\mathrm{T}}\boldsymbol{x} + \boldsymbol{x}^{\mathrm{T}}\boldsymbol{\sigma}\boldsymbol{x}, \tag{32}$$

$$\text{s.t.} \quad \sum_i x_i = 1, \tag{33}$$

$$0 \leq x_i \leq 1, \tag{34}$$

where the expected revenue is

$$\boldsymbol{\mu} = (\mu_1, \mu_2, \ldots, \mu_n)^{\mathrm{T}}, \tag{35}$$

the covariance matrix is

$$\boldsymbol{\sigma} = \begin{pmatrix} \sigma_{11} & \cdots & \sigma_{1n} \\ \vdots & \ddots & \vdots \\ \sigma_{n1} & \cdots & \sigma_{nn} \end{pmatrix}, \tag{36}$$

and the investment ratio is

$$\boldsymbol{x} = (x_1, x_2, \ldots, x_n)^{\mathrm{T}}. \tag{37}$$

Both problems encompass equality and inequality constraints, which can be formulated in the general form shown in Eqs. (1)–(3). Hence, they are amenable to solution via the quantum algorithm proposed in this paper.

On the other hand, the CNOT gate elimination strategy employed in our PCQNN architecture has shown promising results in enhancing computational efficiency while maintaining correctness for the UC problem. We believe that this strategy also holds potential for application to other combinatorial optimization problems, although its effectiveness may vary depending on the specific characteristics of each problem.

In many combinatorial optimization problems, certain variables or constraints may exhibit a degree of independence or weak correlation, similar to the operational decoupling observed in the UC problem. By identifying and exploiting such structural features, it may be possible to apply a similar CNOT gate elimination approach to simplify the quantum circuit and improve computational performance. For instance, in problems such as the traveling salesman problem (TSP) or the

knapsack problem, where certain elements or decisions can be processed independently, a tailored CNOT gate elimination strategy could potentially lead to more efficient quantum solutions.

However, it is important to note that the success of this strategy is not guaranteed for all combinatorial optimization problems. The effectiveness of CNOT gate elimination depends on the specific problem structure, the nature of the objective function, and the constraints involved. In some cases, the interdependencies between variables may be too strong to allow for significant simplification without compromising the accuracy of the solution. Therefore, a thorough analysis of each problem's characteristics is necessary to determine the feasibility and potential benefits of applying the CNOT gate elimination strategy.

While the Hamiltonian analysis provides a useful framework for understanding the physical interpretation of our quantum algorithm design, it has certain limitations in fully explaining the CNOT gate elimination approach. These limitations are summarized in the following points.

First, the proposed PCQNN operates within a heuristic framework. Within the NISQ era, heuristic algorithms are typically evaluated according to their empirical efficacy.[22] The Hamiltonian analysis presented here serves only as an auxiliary physical interpretation and does not provide a complete theoretical proof of the effectiveness of the CNOT gate elimination strategy.

Second, removing the CNOT gates between systems simplifies the quantum circuit structure but increases the number of terms in the Hamiltonian of each individual system. This results in a more complex mathematical description, making it challenging to fully capture the trade-offs between circuit simplicity and solution accuracy.

Third, the Hamiltonian analysis presented in this paper is based on a limited data set of instances. To fully validate the generalizability of our approach, further analysis of a broader range of instance datasets is required. This will help in understanding the robustness and applicability of the CNOT gate elimination strategy across different problem scenarios.

Future work should focus on deeper discussions and research into Hamiltonian analysis for more general combinatorial optimization problems. This will involve exploring alternative analytical approaches and conducting extensive experiments to gain a more comprehensive understanding of the quantum circuit's behavior and the impact of CNOT gate elimination on its performance.

4. Simulation results

The d layers of parametrized quantum gates are then ready to go through the closed-loop optimization process with a classical optimizer. The classical optimizer is used to obtain variational parameters θ^* such that the expected function $\langle H\rangle$ is minimized:

$$\theta^* = \operatorname{argmin}\mathcal{H}(\theta), \tag{38}$$

where $\mathcal{H}$ is the expectation value

$$\mathcal{H}(\theta) = \langle\phi(\theta)|H|\phi(\theta)\rangle, \tag{39}$$

with $\phi(\theta)$ the output quantum state after passing the ansatz block of the quantum circuit.

4.1. Exact solution for ten-unit, one constraint

The method is first tested with ten power units with the power balance constraint. The generator's data can be found in Table 2.[15] According to the discussion above, the single layer of the QNN circuit is constructed as shown in Fig. 4. We tested several quantum circuits with different depths and found that when $d = 10$, the solution obtained by quantum computation is slightly different from the solution given by the classical solver, which can be found in Table 3.

Table 2. Data for a ten-unit power system.

i	1	2	3	4	5	6	7	8	9	10
a_i (\$/MW^2)	0.0048	0.00031	0.002	0.00211	0.00398	0.00712	0.0079	0.00413	0.00222	0.00173
b_i (\$/MW)	16.19	17.26	16.60	16.50	19.70	22.26	27.74	25.92	27.27	27.79
c_i (\$)	1000	970	700	680	450	370	480	660	665	670
p_i (MW)	150	150	20	20	25	20	25	10	10	10

Table 3. Data for a ten-unit power system with a penalty parameter of $\lambda_1 = 100$.

L (MW)	**Classical**	**Quantum**	
		$d = 10$	$d = 13$
50	0001010000	0001010000	0001010000
100	0011111000	0011111000	0011111000
200	**0001010001**	0001010010	**0001010001**

When we add three additional layers, the outcomes from quantum computing agree with the optimal solutions derived from classical methods. Hence, we deduce that the QNN circuit possesses superior expressive capabilities when $d = 13$, which suffices for achieving optimal results. We employ 1000 shots for the optimization loop, allowing for the consistent output of a unique result. This implies that the same outcome is reproducible across 1000 measurements, confirming the result's precision and indicating that the solution accuracy is 100%.

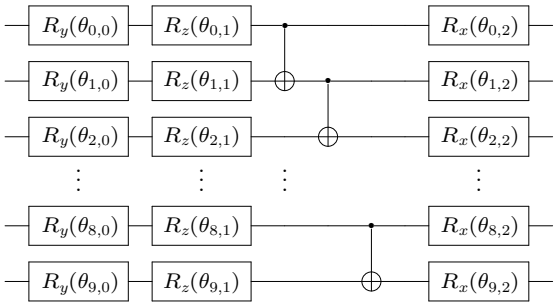


Fig. 4. Diagram of the quantum circuit of the HEA QNN for a ten-unit system and one constraint (one layer).

4.2. Exact solution for five-unit, two constraints

We now examine a power system subject to dual constraints, namely, the power balance constraint and the spare capacity constraint, requiring the use of five auxiliary qubits. Due to the constraints of simulators, when the runtime for more than ten qubits becomes very large, we must reduce the number of units to five, as the total number of qubits utilized is still ten.

In this five-unit power system with dual constraints, auxiliary qubits are employed to represent the relaxation variables. To construct a PCQNN circuit, we can eliminate the CNOT gate connecting the fifth qubit and the sixth qubit, as discussed in Subsection 3.2. The interaction term is diagonal in the tensor product basis, preserving the tensor product state structure; thus, the action of the interaction term remains a tensor product state $|\psi_A\rangle \otimes |\psi_B\rangle$, introducing no entanglement. Therefore, the auxiliary qubits are separate from the others. This configuration is depicted in Fig. 5.

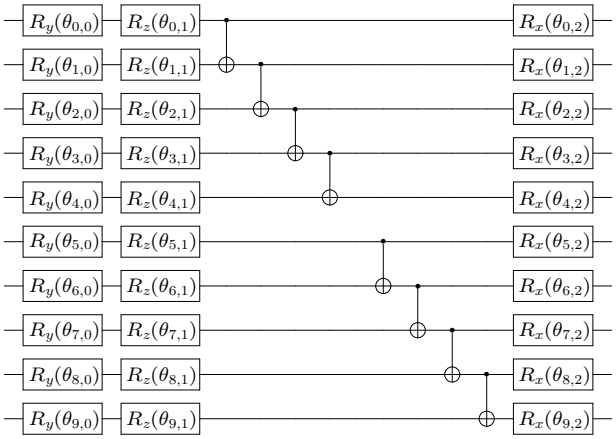


Fig. 5. Diagram of the knowledge-based PCQNN circuit for the five-unit system and double constraints (one layer).

Table 4. Data for the five-unit power system.

i	a_i (\$/MW^2)	b_i (\$/MW)	c_i (\$)	p_i (MW)	$p_{i,\max}$ (MW)
1	0.00175	1.75	0	0.6	0.8
2	0.0625	1.00	0	0.3	0.5
3	0.00834	3.25	0	0.25	0.35
4	0.0025	3.00	0	0.2	0.3
5	0.0025	3.00	0	0.3	0.4

Table 5. Comparison between quantum (including QNN and PCQNN) and classical algorithms for five units and double constraints; the penalty parameters are set to $\lambda_1 = 100$ and $\lambda_2 = 1$.

L (MW)	S (MW)	**HEA QNN**	Probability	Layers	**PCQNN**	Probability	Layers	**Classical**
0.6	0.2	01100	0.83	7	**10000**	1	6	**10000**
0.9	0.2	11000	1	7	11000	1	4	11000
1.1	0.4	11010	1	4	11010	1	4	11010
1.4	0.5	11011	1	2	11011	1	2	11011

Data for the five-unit system can be located in Table 4.[25] The input quantum state is initialized to the all-zero state, denoted by $|0\rangle^{\otimes 10}$. We proceed by employing both the HEA QNN (as shown in Fig. 4) and the PCQNN (as depicted in Fig. 5) for comparative analysis; we also vary the number of layers. The optimization outcomes are presented in Table 5. To confirm the solutions, we obtain optimization results using a classical solver. The findings indicate that the solutions given by the HEA QNN (based on the circuit in Fig. 4) closely match those of the classical solver, the exception being when $L = 0.6$ and $S = 0.2$. In this particular case, the QNN yields a solution of 01100 with a probability of 0.83. In contrast, the PCQNN achieves exact solutions in all cases with a probability of up to 100%. For the scenario with $L = 0.9$ and $S = 0.2$, the QNN requires at least seven layers to achieve an exact solution, whereas the PCQNN only necessitates four layers. Therefore, while ensuring the accuracy of the calculation, we reduced the total number of quantum gates from 273 to 152 and decreased the number of entangling gates from 63 to 32. Hence, the complexity of the circuit is reduced, and the efficiency of the quantum algorithm is improved.

Here, we have discovered a very interesting phenomenon. It is indeed widely accepted that removing CNOT gates negatively impacts the expressiveness of a quantum circuit. From this perspective, the HEA QNN — being structurally more expressive — should outperform the PCQNN after CNOT gates are removed. However, as can be seen in Table 5, the PCQNN converges to a more optimal result than the HEA QNN. In response to this, we conducted an in-depth investigation and analysis.

In quantum machine learning, the expressibility of QNNs is a crucial factor in quantum machine learning tasks. In previous studies, researchers have conducted quantitative analyses of the expressiveness of QNNs. Specifically, the Kullback–Leibler (KL) divergence can be used to characterize the

strength of a QNN's expressiveness. For details, please refer to Ref. [26]. Further elaboration is omitted here.

In general, the stronger the expressiveness of the proposed QNN, the higher the likelihood that quantum machine learning can find the global optimal solution. Please note that the phrase used here is "the higher the likelihood", rather than a guarantee.

Although removing CNOT gates from an HEA QNN diminishes its expressiveness, given the same number of iterative layers, an HEA QNN has stronger expressiveness than a PCQNN. As we mentioned above, stronger expressiveness implies a higher likelihood of finding the global optimal solution. In other words, albeit with a low probability, it is possible that an HEA QNN may fail to find the optimal solution while a PCQNN succeeds. This is precisely the result shown in Table 5.

Regarding the seemingly counterintuitive phenomenon that PCQNN outperforms HEA QNN in some cases, we have conducted a thorough analysis and reproduced all the simulation experiments presented in the paper. Our investigation reveals that the quality of the convergence results is influenced by a variety of factors, such as the setting of penalty parameters, the randomly chosen initial parameter vectors, the number of iterations, the convergence criteria, and the choice of optimizer, rather than being solely determined by the expressiveness of the QNNs.

In our research, we found that when the HEA QNN experiments were repeated multiple times, the HEA QNN was able to converge to the optimal solution with a probability of 100% using a six-layer structure, and this was achieved in most cases. This phenomenon aligns with our expectations. The result of 0.83 may be due to the random selection of initial values, which prevented it from converging to the optimal solution. At that time, only one simulation experiment was conducted, and the result was recorded, which may have affected the representativeness of the result.

However, in terms of computational efficiency, i.e., the required optimization time, PCQNN can undoubtedly reach the optimal solution more quickly. This is because it requires fewer quantum gates. If such experiments were conducted in a real physical system, this difference would become even more pronounced. In practice, multiqubit gate operations take more time than single-qubit gate operations, and a quantum circuit with a larger number of quantum gates inevitably consumes more time.

If we define the expressiveness of a QNN as the number of unitaries it can express when traversing the circuit parameters, then a QNN with stronger expressiveness will have a larger number of unitaries. This means that it may take longer to search for the unitaries that can globally minimize the loss function, but the probability of a successful search is higher. Conversely, if the QNN has weaker expressiveness, although there are fewer unitaries to search through, the probability of successfully finding the unitaries that minimize the loss function is also lower.

In the example dataset of this paper, the final state corresponding to the optimal solution is unique and can be reached by a PCQNN, which allows the PCQNN to converge to the optimal solution faster than the HEA QNN. The lower loss value to which the PCQNN converges is related to the randomly chosen initial parameters in the simulation experiments. When multiple repeated experiments are conducted under the same initial parameters, both HEA QNN and PCQNN can achieve the same loss value and find the optimal solution. However, when dealing with more complex datasets, HEA QNN may exhibit better convergence performance, but at the same time, its optimization time is likely to be longer than that of PCQNN. In the future, we can conduct more simulation experiments on this basis to verify our conjecture.

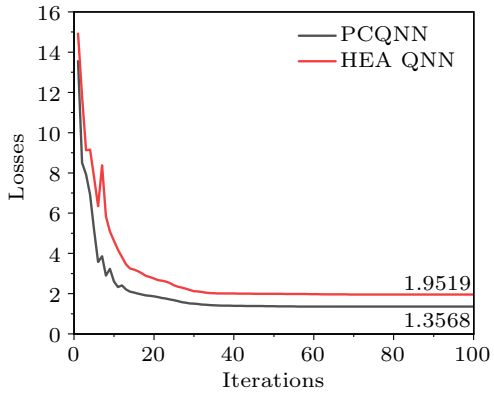


Fig. 6. Losses as a function of iteration number for $L = 0.9$ and $S = 0.2$ for the PCQNN and HEA QNN implemented using four-layer circuits.

On the other hand, the convergence speed can be analyzed based on the losses. Figure 6 illustrates the losses as a function of the iteration number. With constraints of $L = 0.9$ and $S = 0.2$, we compare the performances of four-layer quantum circuits implementing both the PCQNN and the HEA QNN. For the PCQNN, the losses converge at around 28 iterations, while for the HEA QNN, the losses begin to converge at around iteration 33. It is evident that the PCQNN converges faster than the HEA QNN and achieves a lower loss value (~ 1.95 for the HEA QNN and ~ 1.36 for the PCQNN). Thus, for this specific problem, the PCQNN demonstrates two advantages over the HEA QNN: faster convergence speed and a more accurate solution. This demonstrates that the PCQNN can reduce the depth of the quantum circuit while maintaining precision, thereby enhancing computational efficiency. Furthermore, as the number of units increases, we will inevitably encounter a greater number of inequality constraints. The proposed scheme offers a divisible quantum circuit, which opens up possibilities for distributed quantum computing.

Overall, the expressiveness of QNNs has not affected the correctness of the results in this paper, nor has it led to any in-

consistencies in the statements. In the process of using QNNs to solve the UC problem, our goal was not only to find the optimal solution to the problem but also to complete the task with higher computational efficiency. This goal has indeed been achieved through the use of the PCQNN.

5. Conclusions

We proposed a QNN algorithm designed to address the UC problem. Our approach involves transforming the UC problem into a QUBO problem, which can be precisely resolved by the QNN quantum–classical hybrid algorithm. In the case of a UC problem featuring ten generators with a single constraint, the probability of achieving the optimal results is 100%, thanks to the robust expressive capacity of a HEA QNN circuit with 13 repeating layers. However, when dealing with a UC problem that includes five generators and two constraints, we observe that a PCQNN circuit outperforms the HEA QNN algorithm in terms of both accuracy and efficiency. By strategically eliminating entangled gates between unit qubits and auxiliary qubits based on symbolic domain knowledge, we segment the QNN circuit to create a divide-and-conquer quantum algorithm. The PCQNN is a knowledge-based artificial QNN, capable of constructing different elements through independent blocks. This quantum algorithm is not only suitable for the UC problem but also adaptable to a wide array of optimization problems characterized by diverse constraints. In the future, we plan to validate more complex datasets and consider a greater number of units as well as additional constraints, thereby bringing our research problem closer to the actual conditions of power systems.

Acknowledgement

This work was supported in part by the China Postdoctoral Science Foundation (Grant No. 2023M740874).

References

[1] Cheng C P, Liu C W and Liu C C 2000 *IEEE Transactions on Power Systems* **15** 707
[2] Haoyong C, Kaoshe Z and Xifan W 1999 *Proceedings-Chinese Society of Electrical Engineering* **19** 9
[3] Moussouni F, Tran T, Brisset S and Brochet P 2007 *Exhaustive Enumeration (EE) method*, EC Lille, France
[4] Burns R M 1975 *Proc. IEEE Power Eng. Soc. Summer Meeting*
[5] Zhuang F and Galiana F D 1988 *IEEE Transactions on Power Systems* **3** 763
[6] Kazarlis S A, Bakirtzis A and Petridis V 1996 *IEEE Transactions on Power Systems* **11** 83
[7] Cerezo M, Arrasmith A, Babbush R, Benjamin S C, Endo S, Fujii K, McClean J R, Mitarai K, Yuan X, Cincio L, *et al.* 2021 *Nat. Rev. Phys.* **3** 625
[8] Li Y, Hu J, Zhang X M, Song Z and Yung M H 2019 *Advanced Theory and Simulations* **2** 1800182
[9] Farhi E and Harrow A W 2016 arXiv:1602.07674
[10] Li W, Lu Z D and Deng D L 2022 *SciPost Physics Lecture Notes* 061
[11] Kwak Y, Yun W J, Jung S and Kim J 2021 *Twelfth International Conference on Ubiquitous and Future Networks (ICUFN)* (IEEE) pp. 413–416
[12] Wang S, Wang K H, Cheng T, Zhao R S, Ma H Y and Guo S 2024 *Chin. Phys. B* **33** 060310
[13] Xu J, Chen X G, *et al*. 2022 *Chin. Phys. B* **31** 080304
[14] Wang L J, Lin J Y and Wu S 2022 *Chin. Phys. Lett.* **39** 050301
[15] Koretsky S, Gokhale P, Baker J M, Viszlai J, Zheng H, Gurung N, Burg R, Paaso E A, Khodaei A, Eskandarpour R, *et al.* 2021 *IEEE International Conference on Quantum Computing and Engineering (QCE)* (IEEE) pp. 181–187
[16] Mahroo R and Kargarian A 2022 *IEEE Texas Power and Energy Conference (TPEC)* (IEEE) pp. 1–5
[17] Stein J, Jojo J, Farea A, Bucher D, Altmann P and Linnhoff-Popien C 2023 arXiv:2305.08482
[18] Nikmehr N, Zhang P and Bragin M A 2022 *IEEE Transactions on Power Systems* **37** 3592
[19] Yang M, Gao F, Wu G, Gong B, Cao H and Shuang F 2023 *A quantum-aided algorithm for unit commitment problems* **2023** 42
[20] Petros E, Samuel C and Spyros C 2024 arXiv:2404.10693
[21] Elizondo D and Fiesler E 1997 *International Journal of Neural Systems* **8** 535
[22] Shaydulin R, Li C, Chakrabarti S, DeCross M, Herman D, Kumar N, Larson J, Lykov D, Minssen P, Sun Y, *et al.* 2024 *Science Advances* **10** eadm6761
[23] Cui L, Xu Q, Han Z Y and Xu X 2012 *Chin. Phys. Lett.* **29** 037701
[24] Batı M and Ertaş M M 2025 *Physica A* **658** 130268
[25] Selvakumar K, Vijayakumar K and Boopathi C S 2017 *Appl. Sci.* **7** 1127
[26] Sim S, Johnson P D and Aspuru-Guzik A 2019 *Advanced Quantum Technologies* **2** 1900070